THE DYNAMICS OF NITRIC ACID PRODUCTION AND THE FATE OF NITROGEN OXIDES

Armistead G. Russell[+], Gregory J. McRae[*] and Glen R. Cass[x]

Environmental Quality Laboratory 206-40
California Institute of Technology
Pasadena, California 91125

ABSTRACT

A mathematical model is used to study the fate of nitrogen oxides (NO_x) emissions and the reactions responsible for the formation of nitric acid (HNO_3). Model results indicate that the majority of the NO_x inserted into an air parcel in the Los Angeles basin is removed by dry deposition at the ground during the first 24 hours of travel, and that HNO_3 is the largest single contributor to this deposition flux. A significant amount of the nitric acid is produced at night by N_2O_5 hydrolysis. Perturbation of the N_2O_5 hydrolysis rate constant within the chemical mechanism results in redistribution of the pathway by which HNO_3 is formed, but does not greatly affect the total amount of HNO_3 produced. Inclusion of NO_3-aerosol and N_2O_5-aerosol reactions does not affect the system greatly at collision efficiencies, α, of 0.001, but at $\alpha = 0.1$ or $\alpha = 1.0$, a great deal of nitric acid could be produced by heterogeneous chemical processes.

Ability to account for the observed nitrate radical (NO_3) concentrations in the atmosphere provides a key test of the air quality modeling procedure. Predicted NO_3 concentrations compare well with those measured by Platt et al. (1980). Analysis shows that transport, deposition and emissions, as well as chemistry, are important in explaining the behavior of NO_3 in the atmosphere.

[+] Department of Mechanical Engineering

[*] Department of Chemical Engineering, Carnegie-Mellon University, Pittsburgh, Pennsylvania 15213

[x] Environmental Engineering Science Department

1. Introduction

Nitric acid is a major end product of nitrogen oxides emissions. Its presence in the atmosphere can lead to the acidification of rain and fog (Galloway and Likens, 1981; Waldman et al., 1982; Levine and Schwartz, 1982; Liljestrand and Morgan, 1978; Adewuyi and Carmichael, 1982) and to dry deposition (Russell et al., 1984; Liljestrand, 1980; Huebert, 1983). Aerosol nitrates, formed by reaction between nitric acid and either ammonia or preexisting aerosol, are key contributors to the visibility problems observed in cities like Los Angeles and Denver (White and Roberts, 1977; Groblicki et al., 1981). As a result, there is considerable interest in better understanding the mechanisms by which nitric acid is formed in and removed from the atmosphere.

Recent studies of the deposition of nitrogen-containing species and the formation of aerosol nitrates (McRae and Russell, 1984; Russell et al., 1983, 1984; Russell and Cass, 1984) show that an understanding of the fate of nitrogen oxides (NO_x) emissions depends on several poorly understood steps in the nitric acid production cycle. Calculations are sensitive to the treatment of dinitrogen pentoxide (N_2O_5) hydrolysis, dry deposition rates, aerosol scavenging processes, and temporary storage of NO_x in the form of aerosol nitrates and peroxyacetyl nitrate (PAN). The purpose of the present paper is to estimate the relative importance of these key processes to the formation and fate of nitric acid and other major nitrogen-containing pollutants.

A number of different methods may be employed to investigate nitric acid production, notably: smog chamber studies, mathematical models, and atmospheric measurements. Each of these approaches has its individual strengths and weaknesses. Smog chamber studies do not take into account fresh emissions, diffusion, transport and deposition to natural surfaces, although they do allow accurate characterization of the pollutant evolution within a confined air mass. Studies based on atmospheric measurements have the advantage that the air being sampled has been exposed to all of the actual processes affecting pollutant formation. In practice, however, it is hard to follow individual air parcels in the field. In addition, field data usually are taken at ground level, with little or no attention being given to the chemistry and transport processes taking place aloft. Likewise, it is very difficult to separate the effects of transport, chemistry, and emissions from one another given most sets of field experimental data.

Mathematical models, in their many forms, can retain most of the strengths of the two previous methods. All theoretical formulations embody some degree of approximation, and a variety of assumptions must be used. However, if a model can be formulated that performs well when compared to smog chamber and field observations, its use has many advantages as a diagnostic tool for exploring atmospheric processes. These models incorporate descriptions of vertical diffusion, deposition, pollutant emissions and advective transport. By suppressing each of these processes in turn, one can investigate the extent to which particular physical or chemical mechanisms are

responsible for the time rate of change of pollutant concentrations observed at ground-based air monitoring sites. In the present study, a photochemical trajectory model will be used to explore the mechanisms that determine nitric acid concentrations in the atmosphere.

2. Trajectory Model Description

The trajectory model adopted for use in this study is described by Russell et al. (1983), and includes the effects of gas phase chemistry, the formation of nitrate aerosol, emissions, deposition and vertical diffusion. The photochemical mechanism based on McRae et al. (1982) has been augmented with the aerosol nitrate chemistry of Russell et al. (1983). Five additional reactions involving NO_3 have been added:

$$NO_3 + HCHO \xrightarrow{53} HNO_3 + HO_2 + CO \qquad k_{53} = 0.86 \ ppm^{-1} \ min^{-1}$$

$$NO_3 + RCHO \xrightarrow{54} RCO_3 + HNO_3 \qquad k_{54} = 3.6 \ ppm^{-1} \ min^{-1}$$

$$NO_3 + h\nu \xrightarrow{55} 0.7 \ NO_2 + 0.7 \ O + 0.3 \ NO \qquad k_{55} = f(h\nu)$$

$$NO_3 + OLE \xrightarrow{56} RPN \qquad k_{56} = 12.4 \ ppm^{-1} \ min^{-1}$$

$$NO_2 + NO_3 \xrightarrow{57} NO + NO_2 + O_2 \qquad k_{57} = 0.59 \ ppm^{-1} \ min^{-1}$$

Rate constants for the nitrate radical attack on aldehydes and olefins, (OLE), are from Atkinson et al. (1984). The NO_3 photolysis rate used is from Graham and Johnston (1978). The ultimate products of reaction 56 are reported to be nitroxyperoxyalkyl nitrates and dinitrates, abbreviated RPN (Bandow et al., 1980). Tests performed on the model

show that inclusion of reactions 53-57 has little effect on the predictions of ozone, NO or NO_2, but is important to the dynamics of NO_3 and the production of nitric acid. Two other nitric acid-producing reactions are:

$$NO_2 + OH \xrightarrow{18} HNO_3 \qquad k_{18} = 1.52\text{x}10^{4} \ \text{ppm}^{-1} \ \text{min}^{-1}$$

$$N_2O_5 + H_2O \xrightarrow{46} 2HNO_3 \qquad k_{46} = 1.9\text{x}10^{-6} \ \text{ppm}^{-1} \ \text{min}^{-1}$$

The reaction numbers correspond to McRae et al. (1982). Rate constants have been updated to reflect the recommendations of Atkinson and Lloyd (1984) and Baulch et al. (1982).

An evaluation of the chemical mechanism's ability to describe the atmospheric chemistry was accomplished by comparing predictions against a set of smog chamber experiments (Falls and Seinfeld, 1978; McRae, 1981). That comparison showed good agreement between measurements and predictions for both ozone and the measured nitrogen-containing species. Evaluation of the complete trajectory model indicated that it adequately predicts the concentrations of gas phase pollutants, like ozone, and also the production of ammonium nitrate aerosol (see Russell et al., 1983).

3. Nitrogen Fluxes and the Fate of Nitrogen Oxides Emissions

The air quality model was applied to follow the fate of NO_x emissions along a 24-hour trajectory across the Los Angeles basin. The air parcel trajectory used in this analysis is shown in Figure 1, and

passed over the Claremont, California, area at 1600 (PST) on 28 June 1974, the same day for which the initial model verification was accomplished. The air parcel was modeled as a column 1000m high, divided into 10 cells. The cell thicknesses, starting with the ground level cell, were 30m, 50m, 70m, five 100m thick, 150m and 200m. The day was marked by warm temperatures with an elevated inversion and high photochemical activity. Emissions into the air parcel were derived from a spatially resolved emissions inventory of the Los Angeles area. This trajectory was chosen because the Claremont area experiences high ozone levels, and because comparison will be made to NO_3 measurements taken in the same location by Platt et al. (1980).

Results of that model application are shown in Figure 2. The widths of the arrows in Figure 2 represent the magnitude of the integrated net fluxes of nitrogen species between the start of the trajectory and the end of that 24-hour period. These calculations represent net fluxes in the following manner:

$$F_{i\to j}(t) = \sum_m \int_o^t R_m^{i\to j}\ dt - \sum_n \int_o^t R_n^{j\to i}\ dt \qquad (1)$$

where $F_{i\to j}(t)$ is the net flux of nitrogen from species i directly to species j from the beginning of the trajectory to time t, $R_m^{i\to j}$ is the instantaneous flux of nitrogen from species i to j by reaction m and $R_n^{j\to i}$ is similarly the flux from species j to i by reaction n. The summation is taken over all pertinent reactions. These results, of course, depend on the trajectory chosen and on the meteorology of the particular day studied, but they do indicate the general magnitude of

each pathway. From Figure 2 it is seen that emissions of NO comprise about 97% of the flux of NO_x into the system, the remaining 3% being NO_2. The NO is quickly oxidized to NO_2 (the net flux between species is shown), with very little nitrogen deposited out as NO. NO_2 then reacts to form a variety of products: 13% is converted directly to HNO_3, 47% forms PAN, 13% NO_3, 4% N_2O_5, and 20% is removed by dry deposition at the earth's surface. Three percent of the NO_2 remains in the air parcel at the end of 24 hours. About 25% of the net NO_3 formed combines with NO_2 to form N_2O_5, which hydrolyzes to form HNO_3. Most of the NO_3 reacts with the organics to form HNO_3. Dry deposition removes 43% of the PAN in the first 24 hours, leaving the rest to deposit out in subsequent days or to thermally decompose into NO_2 and the peroxyacetyl radical. Thus PAN can act as a reservoir for NO_2. Since nitric acid is very reactive with most surfaces, it deposits out quickly. Almost 73% of the nitric acid formed is lost by dry deposition. Nitric acid and PAN are found to be the major end products of nitrogen oxides emissions at the end of 24 hours. Additional HNO_3 will be produced the next day from the remaining NO_2 and PAN.

A balance on the nitrogen in the air column, Figure 3, indicates the importance of dry deposition. Fifty-eight percent of the NO_x initially present in the air parcel or emitted along the trajectory has deposited out before reaching the end of the 24-hour trajectory. The high HNO_3 formation rates present in photochemical smog promote rapid nitrogen oxides removal at the ground because the deposition velocity of HNO_3 is higher than for many other NO_x species (Huebert, 1983). In

addition, the smog condition studied here is caused in part by low mixing depths that increase pollutant concentrations adjacent to the ground, accelerating dry deposition processes. A plot of the cumulative deposition along the trajectory shows that 39% of the oxides of nitrogen deposited as HNO_3 (Figure 4). PAN and NO_2 contribute 33% and 24%, respectively, to the dry deposition flux, while particulate ammonium nitrate accounts for only 1%.

4. Nitric Acid Production at Night

A comparison of the rates of the four reactions (18, 46, 53, 54) leading to HNO_3 formation is shown in Figure 5. As expected, most of the daytime production of nitric acid occurs due to the reaction of NO_2 with OH. During daylight hours the NO_3 and N_2O_5 levels are very low because of NO_3 photolysis and NO_3 scavenging by NO (Stockwell and Calvert, 1983). At night a considerable amount of nitric acid may be produced by N_2O_5 hydrolysis and NO_3 reactions with organics. During the 24-hour period studied, OH attack on NO_2 and N_2O_5 hydrolysis, respectively, account for 44% and 24% of the total nitric acid produced. The two NO_3 reactions (53,54), in total, account for 32% of the nitric acid generated, mostly by reaction 54.

Clearly the relative importance of various nitric acid formation pathways is dependant on the accuracy of measured rate data. The rate constant for N_2O_5 hydrolysis, k_{46}, adopted in Table 1 is the value recently measured by Tuazon et al. (1983). Earlier research by Morris and Niki (1973) placed an upper limit on k_{46} that is a factor of 8

higher than used in the present study, and the actual rate could still be smaller than used here. Measurement of that rate constant is plagued by rapid heterogeneous reactions with the surfaces of smog chambers used to study that reaction. Two approaches will be taken to estimate the magnitude of the effect that this uncertainty can have on the production of nitric acid. First, the chemical mechanism itself will be dissected to indicate the approximate functional dependence of overall nitric acid production on each of the key rate constants. Then the trajectory model will be used to conduct a study of the effect of perturbed rate constants on predicted HNO_3 formation routes.

The dynamics of the nighttime NO_3-N_2O_5 system is described by the set of 11 reactions shown in Table 1 and can be studied in spite of the possible uncertainty in the rate constant for reaction 46. Excluding the aerosol reactions, the rate expressions for NO_3 and N_2O_5 using the system in Table 1 become:

$$\frac{d[NO_3]}{dt} = k_7[NO_2][O_3]-k_8[NO_3][NO]-k_{44}[NO_2][NO_3]+k_{45}[N_2O_5]-k_{org}[ORG][NO_3] -k_{57}[NO_2][NO_3] \quad (2)$$

and

$$\frac{d[N_2O_5]}{dt} = k_{44}[NO_2][NO_3]-k_{45}[N_2O_5]-k_{46}[N_2O_5][H_2O] \quad (3)$$

where

$$k_{org}[ORG] = k_{53}[HCHO]+k_{54}[RCHO]+k_{56}[OLE] \quad (4)$$

accounts for the reaction of the organics with NO_3. Both NO_3 and N_2O_5

have short characteristic reaction times, and the pseudo-steady state approximation can be made:

$$[NO_3] = \frac{k_7[O_3][NO_2](k_{45}+k_{46}[H_2O])}{\{k_8[NO]+k_{org}[ORG]+k_{57}[NO_2]\}\{k_{45}+k_{46}[H_2O]\}+k_{46}k_{44}[NO_2][H_2O]} \quad (5)$$

and

$$[N_2O_5] = \frac{k_{44}k_7[NO_2]^2[O_3]}{\{k_8[NO]+k_{org}[ORG]+k_{57}[NO_2]\}\{k_{45}+k_{46}[H_2O]\}+k_{44}k_{46}[NO_2][H_2O]} \quad (6)$$

or

$$[N_2O_5] = \frac{k_{44}\,[NO_2]}{k_{45} + k_{46}\,[H_2O]}\;[NO_3] \quad (7)$$

Further simplification is possible in (5) by noting that $k_{45} >> k_{46}[H_2O]$:

$$[NO_3] = \frac{k_7k_{45}[O_3][NO_2]}{k_8k_{45}[NO]+k_{45}k_{org}[ORG]+k_{57}k_{45}[NO_2]+k_{46}k_{44}[NO_2][H_2O]} \quad (8)$$

The denominator in expression (8) is made up from the four sinks in the N_2O_5 - NO_3 system. The first term is due to NO_3 scavenging by NO, the second to the NO_3 reaction with organics, the third to the reaction with NO_2 to form NO, and the last corresponds to nitric acid production by N_2O_5 hydrolysis.

These steady state expressions can be used to perform an uncomplicated check on the NO_3 concentration values reported by Platt et al. (1980) at Claremont, California. Using the NO_2 (0.05 ppm) and

olefins plus aldehydes (0.04 ppm) values representative of nighttime conditions during Platt et al.'s (1980) experiments, given in Table 2, the magnitudes of the last three terms in the denominator of equation (8) are about 0.3, 0.09, and 5 min^{-2}, respectively. Compared to NO, the NO_2 and olefins plus aldehydes concentrations should be relatively constant with height. NO concentrations at ground level are needed if the first term in the denominator of (8) is to be evaluated. Platt et al. (1980) were unable to measure NO, and Tuazon et al. (1981) report NO concentrations at sunset below the detection limit of 1 ppb at Claremont, California. If 1 ppb is taken as an upper limit on the NO concentration at ground level, the first term in the denominator of (8) is of the order 86 min^{-2}, or much greater than the other terms combined. At that ground level NO concentration, the corresponding NO_3 concentration is 12 ppt. At the other extreme, if the ground level NO concentration is negligible, then the corresponding NO_3 concentration is 211 ppt. That range of NO_3 values brackets the peak NO_3 concentrations measured at ground level by Platt et al. (1980) at Claremont.

Equation (8) next can be used to examine the likely situation at night several hundred meters above the ground. Ozone scavenges the NO aloft, and the stability of the atmosphere at night does not allow surface NO emissions to diffuse upward rapidly. Under those conditions, the NO concentration several hundred meters above the ground should be very low (the trajectory model predicts less than 1×10^{-6} ppm aloft just after sunset). With NO levels very low, the

uncertainty in NO concentration present at ground level is removed, and NO_3 values aloft approaching the NO negligible case of 211 ppt should be present. These predictions derived quickly from a steady state analysis of an approximate nighttime chemical mechanism will be compared to the results of the full trajectory model shortly.

The expressions derived for NO_3 and N_2O_5 can be used to compute the nitric acid production rates at night and also to test the sensitivity of nitric acid production to the uncertainty in the N_2O_5 hydrolysis rate. Nitric acid is produced at night by N_2O_5 hydrolysis (reaction 46) and by two reactions between the organics and NO_3 (reactions 53, 54). Rates for these reactions are, respectively

$$\frac{d[HNO_3]}{dt} = \frac{2\, k_{46}k_{44}k_7[H_2O][O_3][NO_2]^2}{k_{46}k_{44}[NO_2][H_2O]+k_{45}k_8[NO]+k_{45}k_{org}[ORG]+k_{45}k_{57}[NO_2]} \quad (9)$$

and

$$\frac{d[HNO_3]}{dt} = \frac{k_{45}k_7[O_3][NO_2](k_{53}[HCHO]+k_{54}[RCHO])}{k_{46}k_{44}[NO_2][H_2O]+k_{45}k_8[NO]+k_{45}k_{org}[ORG]+k_{45}k_{57}[NO_2]} \quad (10)$$

It is instructive to look at the magnitude of equations (9) and (10) in two regimes: if the NO is about 1 ppb and if the NO is negligible.

Using the species concentrations given in Table 2, with NO concentration at 1 ppb, and $k_{46}=1.9\times10^{-6}$ ppm^{-1} min^{-1}, the dominant route for nitric acid production is reaction 46, producing 4×10^{-5} ppm

min^{-1} of HNO_3 (equation 9) compared to $1x10^{-6}$ ppm min^{-1} by the set of NO_3-organics reactions (equation 10).

At high altitudes the NO concentration is very small, decreasing NO_3 scavenging and increasing HNO_3 production. If the NO concentration is negligible, then the nitric acid production rates by reaction 46 and by the organics-NO_3 reactions (reactions 53 and 54) are increased to $7x10^{-4}$ and $1.9x10^{-5}$ ppm min^{-1} respectively. Note that in the absence of NO, decreasing k_{46} has much less effect on HNO_3 production by N_2O_5 hydrolysis. This is because if $[NO] < 10^{-6}$ ppm and $k_{46}k_{44}[NO_2][H_2O] >> k_{45}k_{org}[ORG]$, then (9) simplifies to

$$\frac{d[HNO_3]}{dt} = 2\, k_7\, [O_3][NO_2] \qquad (11)$$

with no dependence on k_{46}.

An estimate of the importance of the N_2O_5 hydrolysis to the total rate of nitric acid production can be found by comparing the previous calculations to the rate of the NO_2-OH radical reaction at noon. Assuming an NO_2 concentration of 0.100 ppm (Tuazon et al., 1981) and an OH radical level of $2x10^{-7}$ ppm (Chameides and Davis, 1982), daytime nitric acid production is about $3x10^{-4}$ ppm min^{-1}, less than the production of HNO_3 by reaction 46 after sunset at locations where the NO concentration is negligible (e.g. above the surface layer affected by fresh NO emissions).

Next the complete photochemical trajectory model was used to test the sensitivity of nitric acid production to variations in a number of key parameters. A comparison of the amount of nitric acid produced by the various reactions in six different cases is shown in Table 3. The base case reflects the calculations previously described in part 3 of this paper. Rate constants shown in Table 1 were used, and no scavenging of NO_3 and N_2O_5 by aerosols was assumed to take place. In this case, nighttime reactions (reactions 46, 53, and 54) account for 56% of the HNO_3 formed during the 24-hour trajectory, 41% of that by the homogeneous hydrolysis of N_2O_5.

There is some possibility that the value of k_{46} given in Table 1 may be too high. A second set of calculations was executed with k_{46} decreased by an order of magnitude below the value in Table 1. In this case only 6% of the nitric acid is produced by reaction 46. However, reducing k_{46} increases the predicted NO_3 concentrations and thus increases the production of HNO_3 by the reactions involving organics. Still, 47% of the nitric acid is produced by nighttime reactions, and the total nitric acid produced is reduced by only 3% (see Table 3).

Morris and Niki (1973) placed an upper limit on the value of k_{46} equal to 1.5×10^{-5} ppm^{-1} min^{-1}. If this value is used, 44% of the nitric acid is produced by homogeneous hydrolysis of N_2O_5 and 36% by the $OH-NO_2$ daytime reaction. At the other extreme, if k_{46} is set equal to zero, the total nitric acid produced decreases by only 7%, and the nitrate radical reactions with organics now account for 44% of that

produced. The final three columns of Table 3 indicate the possible effect that heterogeneous reactions could have on the production of nitric acid. These reactions will be discussed further in following paragraphs.

The results shown here indicate that the homogeneous hydrolysis of N_2O_5 probably is an important mechanism in the formation of nitric acid in the atmosphere. Reducing the rate constant used from that of Morris and Niki (1973) to that of Tuazon et al. (1983), a factor of eight decrease, lowered the amount of HNO_3 produced via reaction 46 by only 55%. Further reduction of k_{46} by an order of magnitude decreased total nitric acid produced at night by only 18%. In all cases the nitric acid produced at night is a significant fraction of the total. NO_3 - organic reactions also are shown to be an important source of nitric acid in this analysis. Perturbing k_{46} results in a redistribution of the amount of nitric acid produced by each reaction, but the total nitric formed is not as greatly affected (see bottom of Table 3).

5. Prediction of NO_3 Concentrations

As indicated earlier, two key species in explaining the production of HNO_3 are N_2O_5 and NO_3. Unfortunately, there are no ground level measurements of N_2O_5 available and only one set of ambient measurements of NO_3, NO_2 and O_3 (Platt et al., 1980). However, the rapid conversion of NO_3 to N_2O_5, and subsequent rapid decomposition of N_2O_5 should cause NO_2, NO_3 and N_2O_5 to reach equilibrium at night, such that

$$\frac{[NO_3][NO_2]}{[N_2O_5]} = K$$

where $K = 1.2 \times 10^{-3}$ ppm (Tuazon et al., 1984). Other reactions of NO_3 and N_2O_5 would perturb this equilibrium state only slightly because the timescales for the other competitive reactions are significantly longer than those that establish the equilibrium condition. Hence, an ability to correctly predict NO_3 concentrations at night would suggest that N_2O_5 concentrations also have been predicted correctly. A key test of nighttime nitric acid formation calculations at present thus involves comparison of observed and predicted NO_3 concentrations.

The trajectory model employed earlier can be used to estimate the NO_3 concentrations observed at Riverside on 12 September 1979 by Platt et al. (1980). The initial conditions used were the NO_2 (0.08 ppm), H_2O (23200 ppm), O_3 (0.23 ppm) and NO_3 (0.0 ppm) concentrations measured by Platt et al. (1980) at Riverside at 1800 Pacific Daylight Time (PDT). Emissions, again, were derived from a spatially resolved 1974 inventory of the area. Air mass motion at night on this occasion was small, and the nominal motion of the air parcel between 1800 and 2400 hours PDT would have been only 5.6 km. Since the emission inventory and the air parcel characteristics are defined over 5 km by 5 km grids, a horizontal transport distance of only 5.6 km implies that Platt et al.'s (1980) measurements at a fixed site in Riverside can be compared to a short Lagrangian trajectory calculation passing over that site. A comparison of the measured and predicted ground level NO_3

concentrations is shown in Figure 6. The measured peak was 288 ppt and the predicted peak was about 255 ppt, both profiles showing the dramatic rise in NO_3 just after sunset, and then a rapid decline. The predicted concentrations peak about one half hour before the measured concentrations, possibly due to dissociation rates of NO_2 and NO_3 after sunset that are greater than that modeled, or due to transport on a sub-grid scale. The latter is unlikely as the wind velocities during the experiment were not very great, and the measured ozone and nitrogen dioxide concentrations did not change markedly. O_3 and NO_2 predictions and measurements are shown in Figure 7. Predicted and observed ozone concentrations compare quite well. The NO_2 predictions are lower than observed, but the NO_2 trends over time track one another.

In order to account for the rapid decrease in ground level NO_3 concentrations observed after the peak at 1930 hours as shown in Figure 6, the O_3 concentration must decrease and the NO concentration increase. Stockwell and Calvert (1983) used a box model, lacking vertical resolution and vertical diffusion, and achieved this result by greatly increasing NO emissions into their model. However, NO emissions in Los Angeles, in fact, are decreasing at that time of day. There are several key reasons why the trajectory model used here can reproduce the observed NO_3 peak without an NO emissions increase. Emissions into the vertically resolved trajectory model are treated as ground level sources. As night falls the atmosphere stabilizes, which decreases mixing, causing an increase in the ground level NO concentrations. However, the effect of this lowered mixing rate in the

trajectory model is more widespread than its effect on increasing NO concentrations alone and is not equivalent to injecting more NO into a box model. The lowered mixing rate also affects the NO_2 and O_3 loss rate at the ground and slows the downward flux of O_3 from elevations above the ground level cell in the model. Emissions used in this study are derived from a spatially resolved emissions inventory for the Los Angeles basin, from which the emissions density in the Riverside area can be determined. In the trajectory model, deposition fluxes are computed based on the concentration in the bottom cell only. Use of ground level emissions and deposition, coupled with a stably stratified atmosphere at night, leads to a very pronounced NO_3 concentration profile with elevation in the atmosphere, as shown in Figure 8. Figure 8 also indicates the potential importance of nitric acid production aloft, where the NO_3 and N_2O_5 concentrations are predicted to be much greater than those observed at ground level.

The trajectory model can be used to elucidate the important processes affecting the NO_3 concentration at ground level over time. This will be done by systematically removing physical processes, such as mixing, deposition, chemical reaction and emissions of NO, from the trajectory model run that was initiated using the O_3 and NO_2 values that were measured by Platt et al. (1980) at 1800 PDT on 12 September 1979 at Riverside. The results of this analysis are shown in Figure 9. Removing NO emissions increases the NO_3 peak, to about 575 ppt, because NO is a very efficient NO_3 scavenger. Decreasing the N_2O_5 hydrolysis rate constant, k_{46}, by an order of magnitude, again increases the peak

NO_3 concentration to about 830 ppt. Further decreasing k_{46} to zero only increases the NO_3 concentration peak to 1000 ppt. Reduction of the value of k_{46} in the two preceding cases causes a delay in the occurrence of the NO_3 peak because the removal of nitrogen oxides from the system is delayed. Deleting deposition of all species changes the NO_3 profile greatly, increasing the peak NO_3 concentration by about fifty percent relative to the base case.

Vertical mixing has a major effect on the NO_3 concentrations. Trapping the emissions in the bottom cell of the model almost removes the peak, whereas the base case calculation of the atmospheric mixing after sunset increases the peak NO_3 value and pushes the peak to a later time. Reduced vertical mixing in effect traps more NO emissions in the bottom cell of the model, giving an effect that is opposite to that discussed previously for the case where emissions are suppressed.

This brief analysis shows that chemistry alone cannot explain the behavior of NO_3 in the atmosphere. A complete analysis requires including the effects of transport, deposition and emissions. Given detailed data on emissions, meteorology, and O_3 and NO_2 concentrations, a similar analysis could be applied to the data of Noxon et al. (1980).

6. Aerosol-Radical Interactions

Both NO_3 and N_2O_5 possibly could be scavenged by surface reactions with aerosols (Chameides and Davis, 1982). Though the rates of these reactions are unknown, an upper bound can be found from

kinetic theory. The trajectory model can be used to assess the maximum effect of aerosol scavenging.

Possible products of the nitrate radical interaction with aerosols include aerosol nitrate, a sink in the system, or decomposition of the NO_3 into NO_2 and oxygen. N_2O_5 also might decompose into its precursors, react with the aerosol surface to form aerosol nitrate, or, if the N_2O_5 contacts water on the aerosol surface, it could undergo heterogeneous hydrolysis to produce nitric acid. In the following analysis, the aerosol surface reaction with NO_3 will be modeled as a sink for NO_3, the products remaining in the aerosol phase; while N_2O_5 reaction with the aerosol will be assumed to produce nitric acid that could re-enter the gas phase. Thus, the two reactions added to the system are

$$NO_3 + \text{aerosol} \longrightarrow \text{aerosol} \qquad k^*_{NO_3} = f_1(n(d_p))$$

$$N_2O_5 + \text{aerosol} + H_2O \longrightarrow 2HNO_3 + \text{aerosol} \qquad k^*_{N_2O_5} = f_2(n(d_p))$$

where the two rate constants are calculated as functions of the aerosol size distribution function, $n(d_p)$, which determines the aerosol surface area as a function of particle diameter, d_p.

An upper bound for these rate constants can be derived from kinetic theory by calculating the collision rate of the gas molecules with the aerosol surface. Assuming that 100% of the collisions are effective in achieving reaction, these upper limit rate constants are given by (Dahneke, 1983)

$$k_i^* = \int_0^\infty 2\pi D_i \left[\frac{1 + Kn}{\frac{2 Kn (1 + Kn)}{\alpha} + 1}\right] d_p n(d_p) d(d_p) \quad (12)$$

where D_i is the diffusion coefficient of species i, Kn is the Knudsen number based on aerosol size and the mean free path of gaseous species i, and α is the collision efficiency. An estimate of the heterogeneous reaction rate constants in the Los Angeles atmosphere can be found using the measured aerosol size distribution of Table 3 in Whitby et al. (1972). Upper bounds on these rate constants, using α=1, are calculated to be

$$k^*_{NO_3}(\alpha=1) = 2.4 \text{ min}^{-1}$$

$$k^*_{N_2O_5}(\alpha=1) = 1.5 \text{ min}^{-1}$$

Collision efficiencies are both hard to measure and highly dependent on the aerosol surface characteristics. Baldwin and Golden (1979) measured the collision efficiency of N_2O_5 on a sulfuric acid surface to be greater than 3.8×10^{-5}. Chameides and Davis (1982) report measured efficiencies for OH radical-aerosol reactions from less than 10^{-4} to 0.25, the magnitude depending largely on the surface composition. In the present work, the assumed collision efficiency, α, for both N_2O_5 and NO_3-surface reactions will be taken as 10^{-3}, which is between that measured for N_2O_5 on sulfuric acid and the OH interaction with $NaNO_3$ (Jech et al., 1982). The actual rate will vary as the aerosol surface characteristics and size distribution change.

The importance of aerosol scavenging is dependent on the time scales associated with the different sinks in the NO_3-N_2O_5 system. At night, given the species concentrations in Table 2, these sinks and their time scales (given as the NO_3 reaction rate per unit NO_3 concentration) are:

NO Scavenging	$0.03 < k_8[NO] < 30\ min^{-1}$
Organic Reactions	$k_{org}[ORG] \sim 0.10\ min^{-1}$
Aerosol Interaction	$k^*_{NO_3}(\alpha=0.001) \sim 0.004\ min^{-1}$

From these results, aerosol scavenging of NO_3 at night should be important only at very low NO concentrations or at collision efficiencies much higher than the $\alpha = 10^{-3}$ value assumed here. During daylight hours, the losses due to photolysis and NO scavenging are very much greater than the loss due to aerosols.

At night N_2O_5-aerosol reactions can be examined by comparing the time scales for N_2O_5 loss:

Homogeneous Hydrolysis	$k_{46}[H_2O] < 0.04\ min^{-1}$
Aerosol Interaction	$k^*_{N_2O_5}(\alpha=0.001) \sim 0.003\ min^{-1}$

Considering the uncertainties, the time scales associated with the N_2O_5 sinks at night are close. The N_2O_5 homogeneous hydrolysis rate could easily be an order of magnitude lower and the aerosol interaction higher, the conclusion being that N_2O_5-aerosol interactions are

possibly important at night, lowering the concentrations of both NO_3 and N_2O_5 in the atmosphere.

The trajectory model again can be used to explore the effect of aerosols on the oxides of nitrogen system and on the production of nitric acid by adding the last two reactions shown in Table 1. Again the 24-hour trajectory passing through Claremont was modeled, first with the collision efficiency equal to 0.001 and then with α = 0.1 and 1.0. For α = 0.001, little effect is seen on the nitric acid produced when compared to the base case as shown in Table 3. Likewise, with α = 0.001 there is little effect on the NO_3 peak shown in Figure 9. If α= 0.1 or 1.0, the NO_3 peak almost disappears, but a great deal of nitric acid is produced heterogeneously, indicating the importance of aerosol interactions at high collision efficiencies.

9. Conclusions

The photochemical trajectory model used by Russell et al. (1983) was applied to calculations along a 24-hour air parcel trajectory crossing the Los Angeles basin during a day that exhibits summertime high photochemical smog conditions. Ground level dry deposition calculations show that 58% of the nitrogen oxides inserted into the air parcel have deposited at the ground during that 24-hour period. Nitrogen oxides removal is dominated by HNO_3 (39%), PAN (33%), and NO_2 (24%). Much of the nitrogen left in the air column at the end of the 24-hour trajectory is predicted to be associated with NO_2 or PAN.

During the following day, this PAN can either continue to deposit or thermally decompose releasing NO_2.

Significant nitric acid production takes place both at night and during the daytime. For the most probable case studied here (the base case of Table 3), about 56% of the nitric acid produced during a 24-hour urban trajectory traveling across the Los Angeles basin is generated at night by reactions involving NO_3 and N_2O_5. Most of that HNO_3 production at night is due to the NO_3 reaction with higher aldehydes and hydrolysis of N_2O_5. Both pseudo-steady state analysis of the nighttime chemical mechanism and trajectory model results indicate that nitric acid production is slightly sensitive to an order of magnitude decrease in the N_2O_5 homogeneous hydrolysis rate constant, except at high NO levels or if aerosol scavenging is relatively efficient ($\alpha >> 0.001$).

Aerosol interactions with NO_3 should perturb the system only slightly except at very low NO concentrations, or if the aerosol collision efficiency is high. N_2O_5 interactions with aerosols are more important than NO_3-aerosol reactions at the same collision efficiency, an effect magnified by any decrease in the N_2O_5 homogeneous hydrolysis rate constant. Heterogeneous reactions on aerosols may be important both in the formation of nitric acid, and as a sink for N_2O_5.

An analysis of the possible effects of uncertainties in the N_2O_5 homogeneous hydrolysis rate constant shows that the effect of this uncertainty is much different near the ground than at several hundred

meters above the ground. Many of the perturbations used to estimate the effect of uncertainties within the trajectory model cause a redistribution of the mechanism by which nitric acid is formed but do not affect the total amount of nitric acid produced greatly during a 24-hour period (see the bottom of Table 3).

The nitrate radical, NO_3, is a key species in the mechanism producing HNO_3 by N_2O_5 hydrolysis. The behavior of NO_3 predicted by the trajectory model used here compares well with field observations, and is consistent with known emission rates and atmospheric dynamics in the Los Angeles area. Results indicate that simultaneous calculation of dry deposition, emissions, chemistry, and vertical transport is needed to reproduce Platt et al.'s (1980) observations and that atmospheric measurements made at fixed ground level monitoring sites must be interpreted very carefully if one is to correctly capture the effect of transport processes on atmospheric chemical dynamics.

Acknowledgements: This work was supported, in part, by a grant from the Andrew W. Mellon Foundation and by gifts to the Environmental Quality Laboratory. The California Air Resources Board supported AGR and recent calculations under Agreement A2-150-32.

References

Adewuyi, Y.G. and Carmichael, G.R. (1982) "A Theoretical Investigation of Gaseous Absorption by Water Droplets from SO_2-HNO_3-NH_3-CO_2-HCL Mixtures," Atmospheric Environment, 16, 719-729.

Atkinson, R., Plum, C.N., Carter, W.P., Winer, A.M. and Pitts, J.N., Jr. (1984) "Rate Constants for the Gas Phase Reactions of NO_3 Radicals with a Series of Organics in Air at 298 ± 1 K," J. Phys. Chem., 88 1210-1215.

Atkinson, R. and Lloyd, A. C. (1984) "Evaluation of Kinetic and Mechanistic Data for Modeling of Photochemical Smog," J. Phys. Chem. Ref. Data, 13 315-444.

Baldwin, A.C. and Golden, D.M. (1979) "Heterogeneous Atmospheric Reactions: Sulfuric Acid Aerosols as Tropospheric Sinks," Science, 206, 562-563.

Bandow, H., Okuda, M., Akimoto, H. (1980) "Mechanism of the Gas-Phase Reactions of C_3H_6 and NO_3 Radicals," J. Phys. Chem., 84, 3604-3608.

Baulch, D.L., Cox, R.A., Crutzen, P.J., Hampson, R.F., Kerr, J.A., Troe, J. and Watson, R.T. (1982) "Evaluated Kinetic and Photochemical Data for Atmospheric Chemistry: Supplement 1," J. Phys. Chem. Ref. Data, 11, 327-496.

Chameides, W.L. and Davis, D.D. (1982) "The Free Radical Chemistry of Cloud Droplets and its Impact on the Composition of Rain," J. Geophys. Res., 87, 4863-4877.

Dahneke, B. (1983) "Simple Kinetic Theory of Brownian Diffusion in Vapors and Aerosols," in Theory of Dispersed Multiphase Flow. R. Meyer, Ed., Academic Press, New York.

Falls, A.H. and Seinfeld, J.H. (1978) "Continued Development of a Kinetic Mechanism for Photochemical Smog," Env. Sci. Technol., 12, 1398-1406.

Galloway, J.N. and Likens, G.E. (1981) "Acid Precipitation: The Importance of Nitric Acid," Atmospheric Environment, 15, 1081-1085.

Graham, R.A. and Johnston, H.S. (1978) "The Photochemistry of NO_3 and the Kinetics of the N_2O_5-O_3 System," J. Phys. Chem., 82, 254-268.

Groblicki, P.J., Wolff, G.T. and Countess, R.J. (1981) "Visibility Reducing Species in the Denver "Brown Cloud", Part I. Relationships Between Extinction and Chemical Composition," Atmospheric Environment, 15, 2473-2484.

Huebert, B.J. (1983) "Measurements of the Dry Deposition Flux of Nitric Acid Vapor to Grasslands and Forest," in Precipitation Scavenging, Dry Deposition, and Resuspension. Pruppacher, H.R., Semonin, R.G. and Slinn, W.G.N., coordinators, Elsevier, New York.

Jech, D.D., Easley, P.G., and Krieger, B.B. (1982) "Kinetics of Reactions Between Free Radicals and Surfaces (Aerosols) Applicable to Atmospheric Chemistry," in Heterogeneous Atmospheric Chemistry, D.R. Schryer, Ed., American Geophysical Union, Washington, D.C. 107-121.

Levine, S.Z. and Schwartz, S.E. (1982) "In-cloud and below-cloud scavenging of nitric acid vapor," Atmospheric Environment, 16, 1725-1734.

Liljestrand, H.M. and Morgan, J.J. (1978) "Chemical Composition of Acid Precipitation in Pasadena, California," Env. Sci. Technol., 12 1271-1273.

Liljestrand, H.M. (1980) "Atmospheric Transport of Acidity in Southern California by Wet and Dry Mechanisms" Ph.D. thesis, California Institute of Technology, Pasadena, California.

Malko, M.W. and Troe, J. (1983) "Analysis of the Unimolecular Reaction $N_2O_5 + M \quad NO_2 + NO_3 + M$," Int. J. Chem. Kinetics, 14, 399-416.

McRae, G.J. (1981) "Mathematical Modeling of Photochemical Air Pollution," Ph.D. thesis, California Institute of Technology, Pasadena, California.

McRae, G.J., Goodin, W.R. and Seinfeld, J.H. (1982) "Development of a Second Generation Mathematical Model for Urban Air Pollution: I Model Formulation," Atmospheric Environment, 16, 679-696.

McRae, G.J. and Russell, A.G. (1984) "Dry Deposition of Nitrogen-Containing Species," in Deposition Both Wet and Dry, B.B. Hicks, Ed., Acid Precipitation Series-Vol 4, Butterworth, Boston, 153-193.

Morris, E.D. and Niki, H. (1973) "Reaction of Dinitrogen Pentoxide with Water," J. Phys. Chem., 77, 1929-1932.

Noxon, J.F., Norton, R.B. and Marovich, E. (1980) "NO_3 in the Troposphere," Geophys. Res. Lett., 7, 125-128.

Platt, U., Perner, D., Winer, A.M., Harris, G.W. and Pitts, J.N. (1980) "Detection of NO_3 in the Polluted Troposphere by Differential Optical Absorption," Geophys. Res. Lett., 7, 89-92.

Russell, A.G., McRae, G.J. and Cass, G.R. (1983) "Mathematical Modeling of the Formation and Transport of Ammonium Nitrate Aerosol," Atmospheric Environment, 17, 949-964.

Russell, A.G. and Cass, G.R. (1984) "Acquisition of Regional Air Quality Model Validation Data for Nitrate, Sulfate, Ammonium Ion and Their Precursors," Atmospheric Environment, 18, 1815-1827.

Russell, A.G., McRae, G.J. and Cass, G.R. (1984) "Acid Deposition of Photochemical Oxidation Products - A Study Using a Lagrangian Trajectory Model," from Air Pollution Modeling and Its Application III, C. DeWispelaere Ed., Plenum Publishing Corporation, New York.

Stockwell, W.R. and Calvert, J.G. (1983) "The Mechanism of NO_3 and HONO Formation in the Nighttime Chemistry of the Urban Atmosphere," J. Geophys. Res., 88, 6673-6682.

Tuazon, E.C., Winer, A.M. and Pitts, J.N., Jr. (1981) "Trace Pollutant Concentrations in a Multiday Smog Episode in the California South Coast Air Basin by Long Path Length Fourier Transform Infrared Spectroscopy," Env. Sci. Technol., 15, 1232-1237.

Tuazon, E.C., Atkinson, R., Plum, C.N., Winer, A.M. and Pitts, J.N., Jr. (1983) "The Reaction of Gas Phase N_2O_5 with Water Vapor," Geophys. Res. Lett., 10, 953-956.

Tuazon, E.C., Sanhueza, E., Atkinson, R., Carter, W.P.L., Winer, A.M. and Pitts, J.N., Jr. (1984) "Direct Determination of the Equilibrium Constant at 298K for the NO_2+NO_3 N_2O_5 Reactions," J. Phys. Chem., 88, 3095-3098.

Waldman, J.M., Munger, J.W., Jacob, D.J., Flagan, R.C., Morgan, J.J. and Hoffmann, M.R. (1982) "Chemical Composition of Acid Fog," Science, 218, 677-680.

Whitby, K.T., Husar, R.B. and Liu, B.Y.H. (1972) "The Aerosol Size Distribution of Los Angeles Smog," J. Colloid Interface Sci., 39, 177-204.

White, W. H. and Roberts, P.T. (1977) "On the Nature and Origins of Visibility Reducing Species in the Los Angeles Basin," Atmospheric Environment, 11, 803-812.

TABLE 1

Major Reactions in the NO_3-N_2O_5 System at Night

REACTION	RATE CONSTANT @ 298 K (ppm min units)	REFERENCE
$NO_2 + O_3 \xrightarrow{7} NO_3$	$k_7 = 0.05$	1
$NO + NO_3 \xrightarrow{8} 2NO_2$	$k_8 = 29560$	1
$NO_2 + NO_3 \xrightarrow{44} N_2O_5$	$k_{44} = 2510$	2
$N_2O_5 \xrightarrow{45} NO_2 + NO_3$	$k_{45} = 2.9$	1,3
$N_2O_5 + H_2O \xrightarrow{46} 2HNO_3$	$k_{46} = 1.9 \times 10^{-6}$	4
$NO_3 + HCHO \xrightarrow{53} HNO_3 + HO_2 + CO$	$k_{53} = 0.86$	5
$NO_3 + RCHO \xrightarrow{54} RCO_3 + HNO_3$	$k_{54} = 3.6$	5,6
$NO_3 + OLE \xrightarrow{56} RPN$[8]	$k_{56} = 12.4$	5,7,9
$NO_2 + NO_3 \xrightarrow{57} NO + NO_2 + O_2$	$k_{57} = 0.59$	10
N_2O_5 + aerosol $\longrightarrow 2\ HNO_3$	$\alpha k^*_{N_2O_5}$	11
NO_3 + aerosol $\longrightarrow$ aerosol	$\alpha k^*_{NO_3}$	11

1 - Baulch et al. (1982)
2 - Tuazon et al. (1984)
3 - Malko and Troe (1982)
4 - Tuazon et al. (1983)
5 - Atkinson et al. (1984)
6 - The rate constant used for the NO_3 reaction with higher aldehydes is that measured for acetaldehyde.
7 - The value used for the rate constant of the NO_3 reaction with olefins is that measured for the NO_3 reaction with propene.
8 - The ultimate products of reaction 56 are reported to be nitroxyperoxyalkyl nitrates and dinitrates (Bandow et al., 1980).
9 - Bandow et al. (1980)
10 - Atkinson and Lloyd (1984)
11 - See text

TABLE 2

Species Concentration Used in Analysis

SPECIES	CONCENTRATION (PPM)
NO (average)	1×10^{-4}[a]
NO_2	0.05[b]
O_3	0.15[b]
H_2O	2×10^{4}[b]
HCHO	0.020[c]
RCHO	0.020[d]
OLE	0.001[a]
NO (ground level)	1×10^{-3}[c]
NO (above inversion)	1×10^{-6}[a]

[a] Value taken from trajectory model calculations used in this study at 19:00 PST.

[b] Value representative of those measured by Platt et al. (1980).

[c] Value representative of those measured by Tuazon et al. (1981).

[d] Concentration of higher aldehydes set equal to that of formaldehyde.

TABLE 3

Percent of Total Nitric Acid Produced by Each Reaction
Along a 24-hour Trajectory

REACTION STEP PRODUCING HNO_3	BASE CASE	k_{46} DECREASED BY 10X	k_{46} of MORRIS & NIKI	$k_{46}=0$	AEROSOL SCAVENGING (α=0.001)	(α= 0.1)	(α=1.0)
NO_2 + OH (18)	44%	53%	36%	56%	44%	37%	29%
N_2O_5 + H_2O(g)(46)	24%	6%	44%	0%	22%	5%	tr*
NO_3 + HCHO (53)	4%	7%	2%	7%	4%	1	tr
NO_3 + RCHO (54)	28%	34%	18%	37%	28%	11%	4%
N_2O_5 + AEROSOL					2%	46%	67%
Percent of base case nitric acid produced	100%	97%	117%	93%	101%	114%	124%

* tr = trace amount, less than 1%

Figure Captions

Figure 1 — Trajectory path used in analyzing the nitrogen oxides in the Los Angeles basin, June 28, 1974.

Figure 2 — Schematic representation of the net flux between nitrogen oxides species, including reaction paths for aerosol nitrate (NIT) formation. The width of these arrows indicates the magnitude of the net flux during the base case 24-hour trajectory simulation.

Figure 3 — Nitrogen balance on the air column illustrating the relative contributions, F(n), from initial conditions, emissions and removal by dry deposition.

Figure 4 — Cumulative dry deposition of oxidized nitrogen air pollutants along a 24-hour trajectory in the Los Angeles area, in mg N per m^2 of surface area at the bottom of the moving air column.

Figure 5 — Diurnal variation in the contribution of different reaction pathways to the formation of gas phase nitric acid. The two reactions (53 and 54) between NO_3 and organics have been added together for display purposes.

Figure 6 — Predicted and measured NO_3 concentrations at Riverside, September 12, 1979.
---- Predicted
\+ Measured (Platt et al. 1980)

Figure 7 — Predicted and measured O_3 and NO_2 concentrations at Riverside, September 12, 1979.
---- Predicted
x Measured NO_2 (Platt et al. 1980)
o Measured O_3 (Platt et al. 1980)

Figure 8 — Predicted vertical NO_3 concentration profile at 1900 (PDT) on September 12, 1979. Air parcel is located at Riverside.

Figure 9 — Predicted NO_3 concentrations at Riverside, September 12, 1979 for the base case and for several perturbations from the base case.

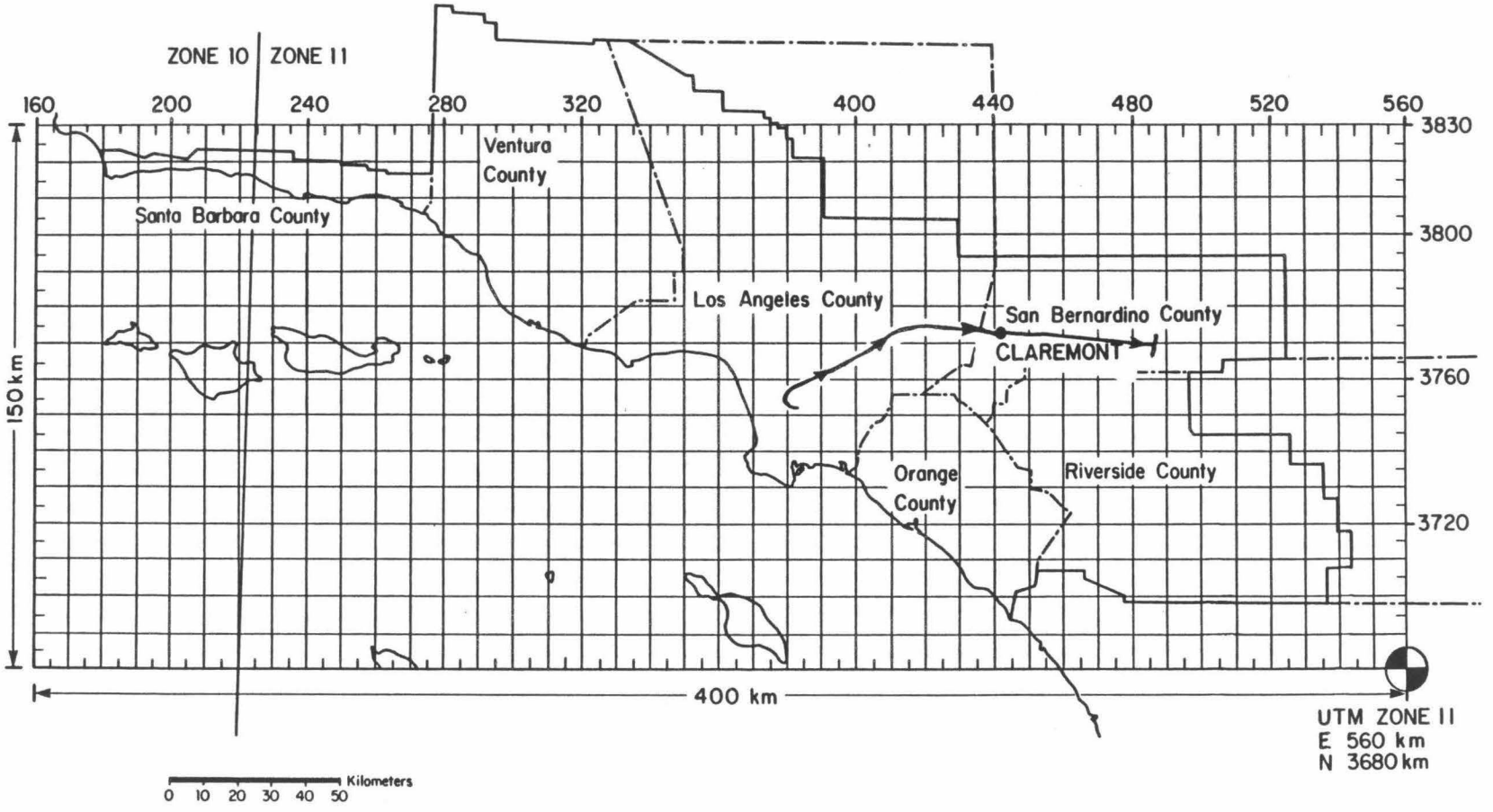
ZONE 10
ZONE 11
160
200
240
280
320
400
440
480
520
560
3830
3800
3760
3720
150 km
Ventura County
Santa Barbara County
Los Angeles County
San Bernardino County
CLAREMONT
Orange County
Riverside County
400 km
UTM ZONE 11
E 560 km
N 3680 km
Kilometers
0 10 20 30 40 50

FIGURE 1

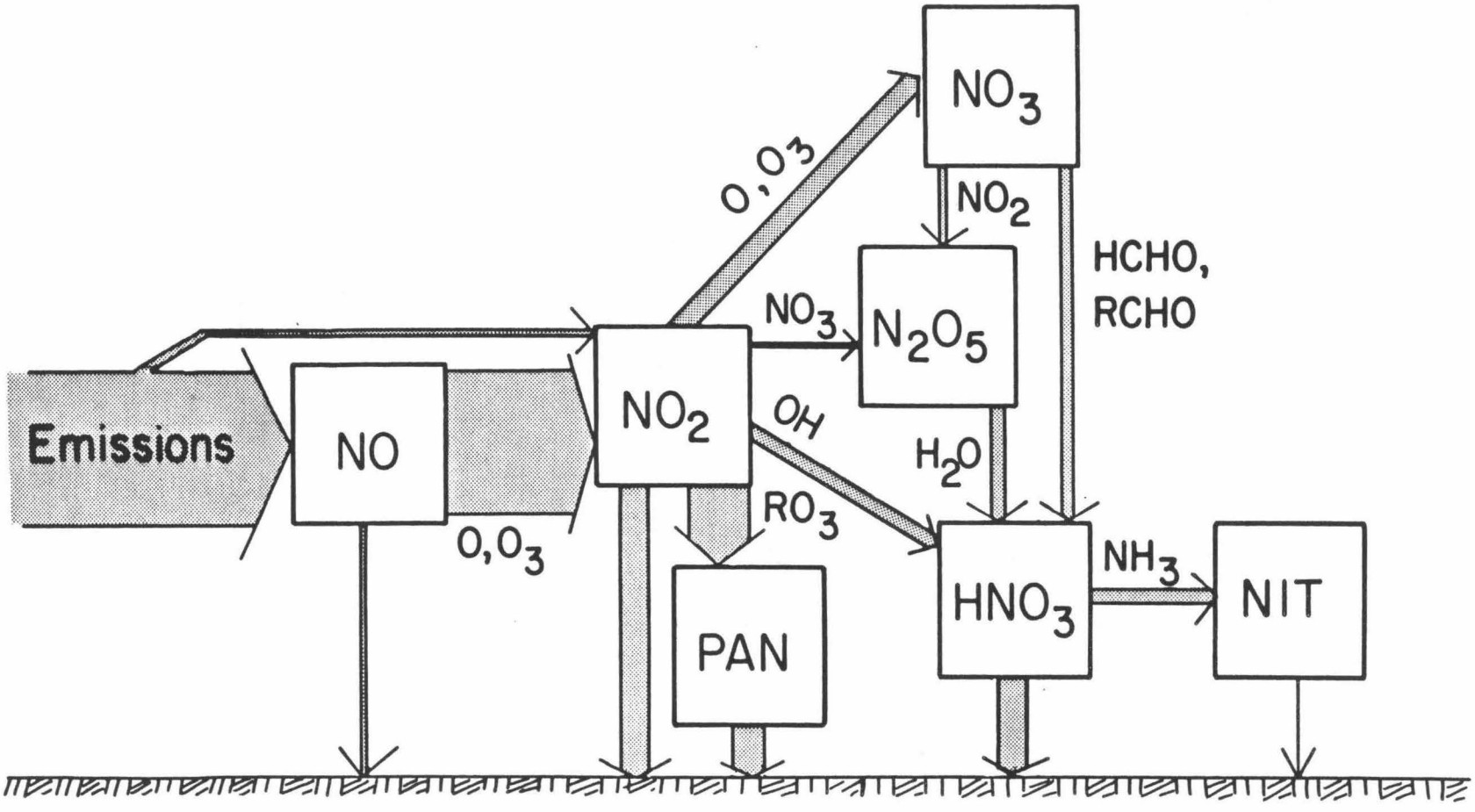
Emissions
NO
O, O_3
NO_2
O, O_3
NO_3
NO_2
NO_3
N_2O_5
OH
H_2O
HCHO,
RCHO
RO_3
PAN
HNO_3
NH_3
NIT

FIGURE 2

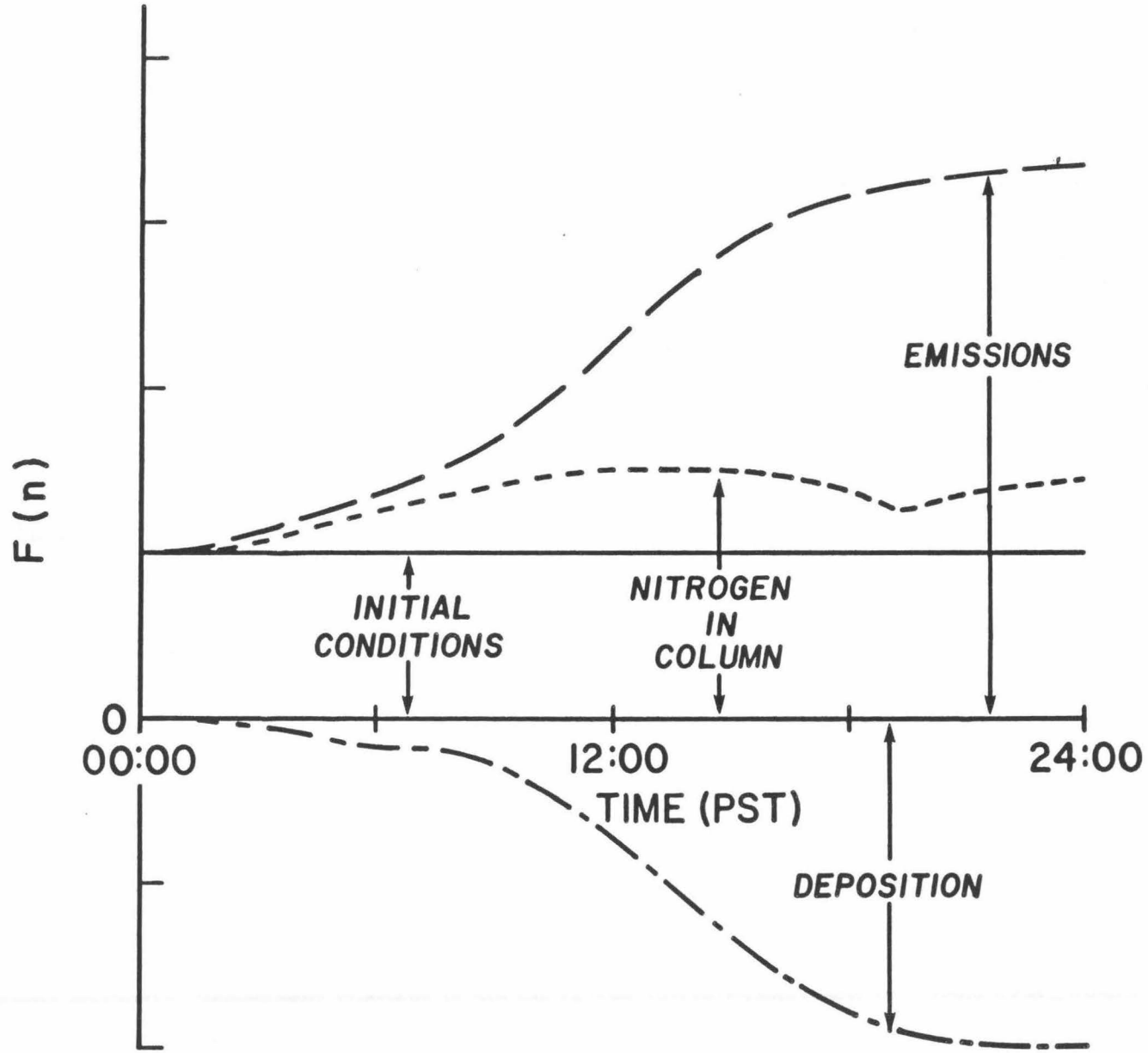
F (n)
EMISSIONS
INITIAL
CONDITIONS
NITROGEN
IN
COLUMN
0
00:00
12:00
24:00
TIME (PST)
DEPOSITION

FIGURE 3

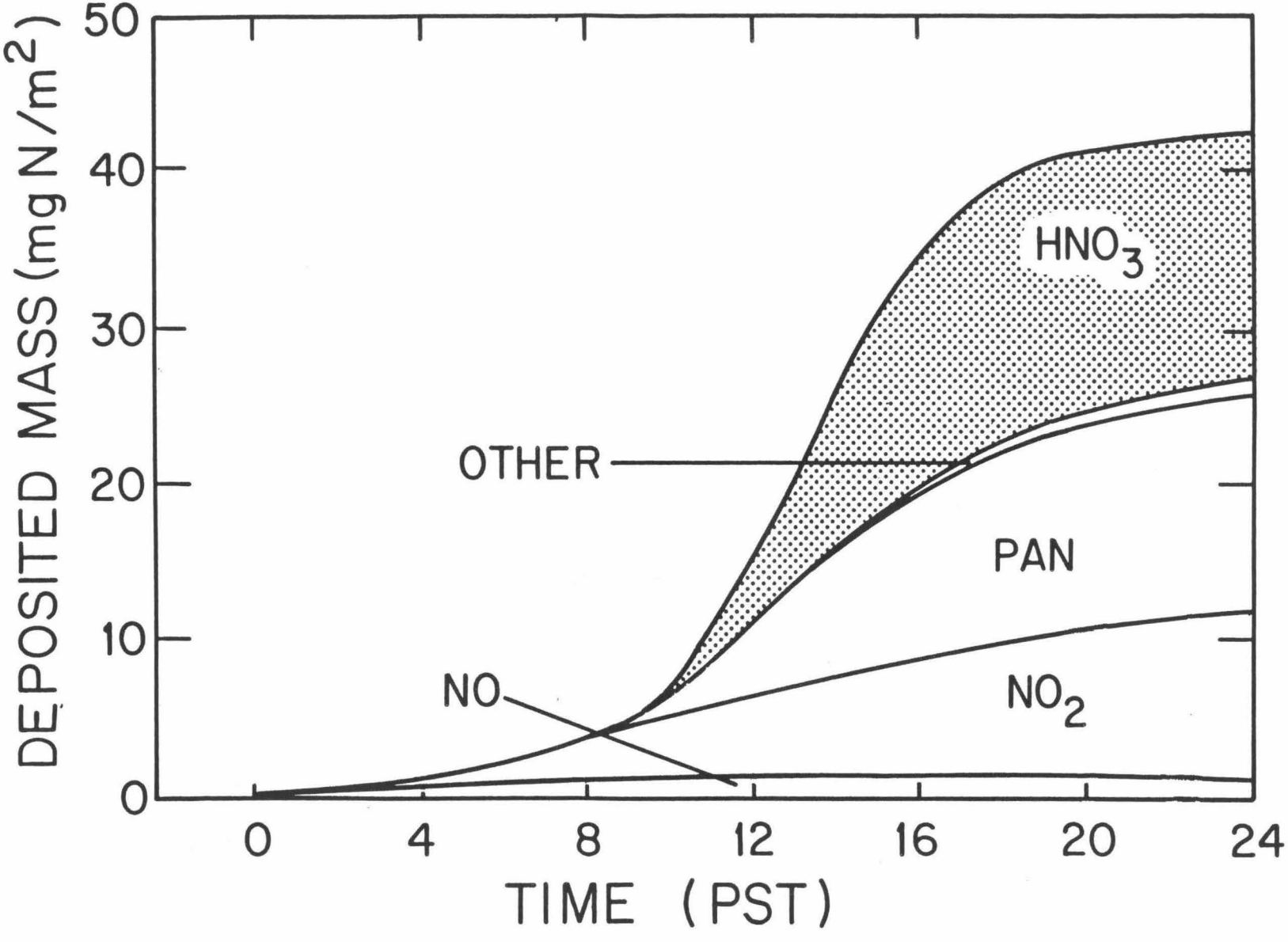
DEPOSITED MASS (mg N/m2)
50
40
30
20
10
0
0
4
8
12
16
20
24
TIME (PST)
HNO3
OTHER
PAN
NO
NO2

FIGURE 4

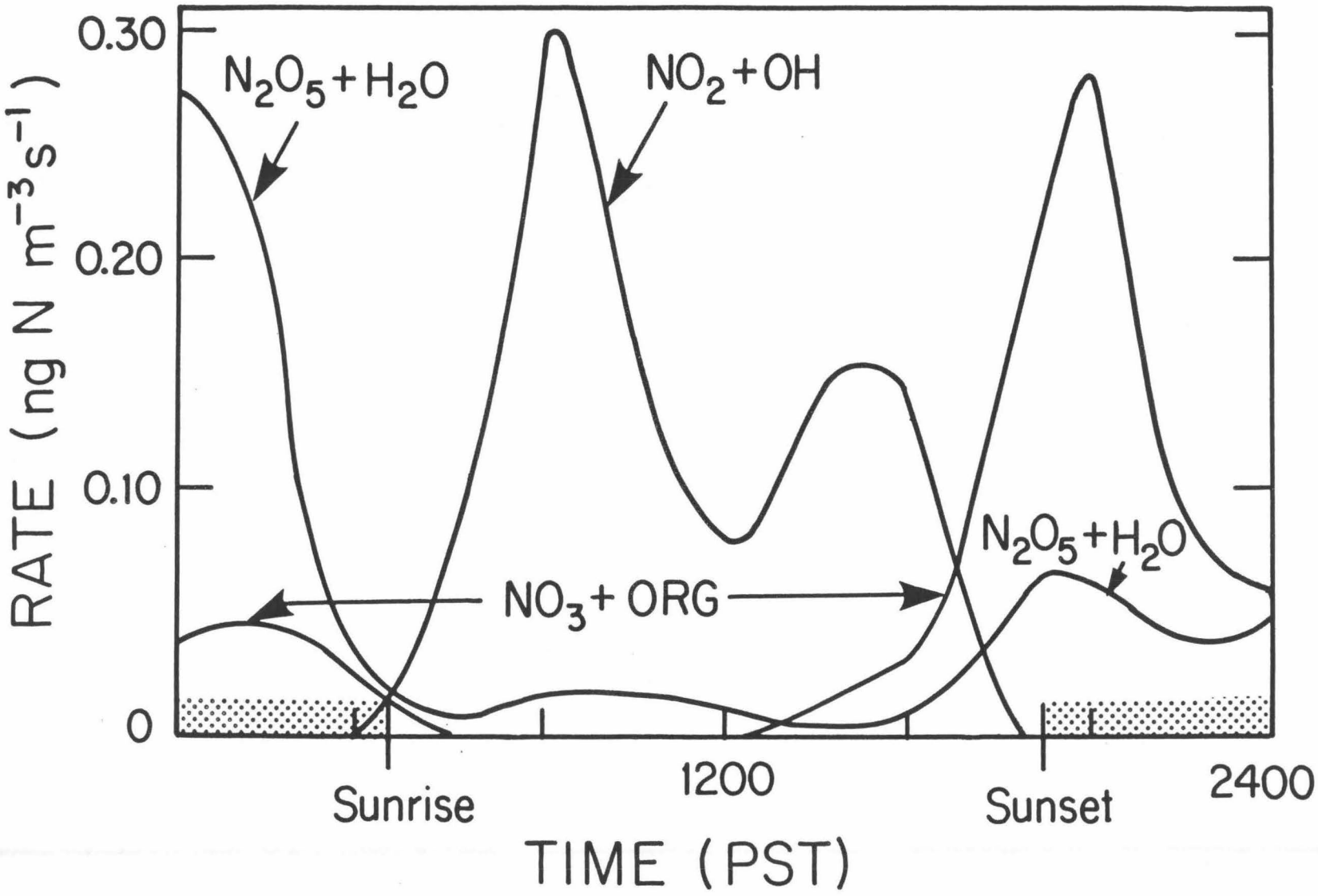
0.30
0.20
0.10
0
RATE (ng N m^{-3}s^{-1})
$N_2O_5+H_2O$
NO_2+OH
NO_3+ORG
$N_2O_5+H_2O$
Sunrise
1200
Sunset
2400
TIME (PST)

FIGURE 5

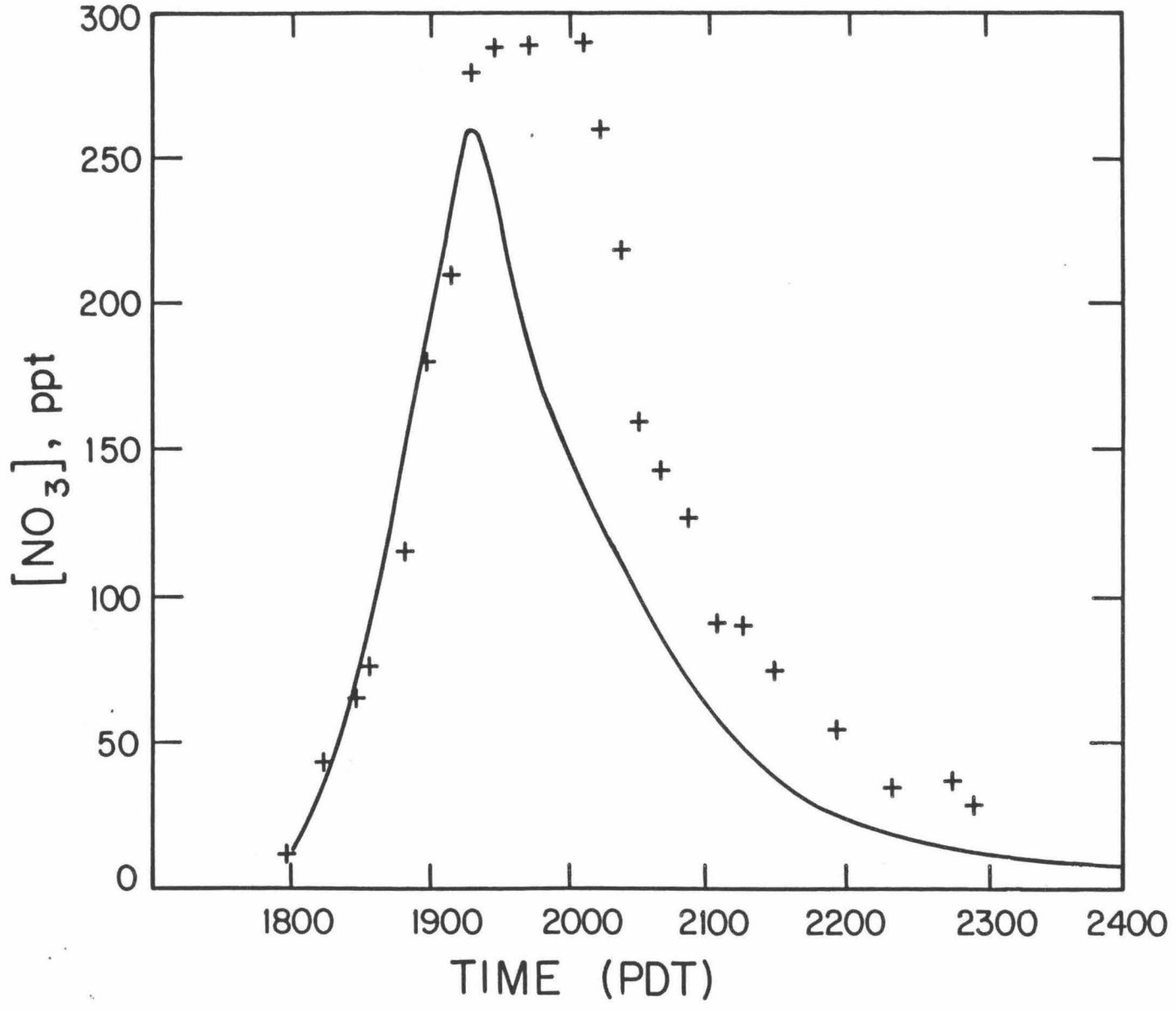
300
250
200
150
100
50
0
[NO3], ppt
1800
1900
2000
2100
2200
2300
2400
TIME (PDT)

FIGURE 6

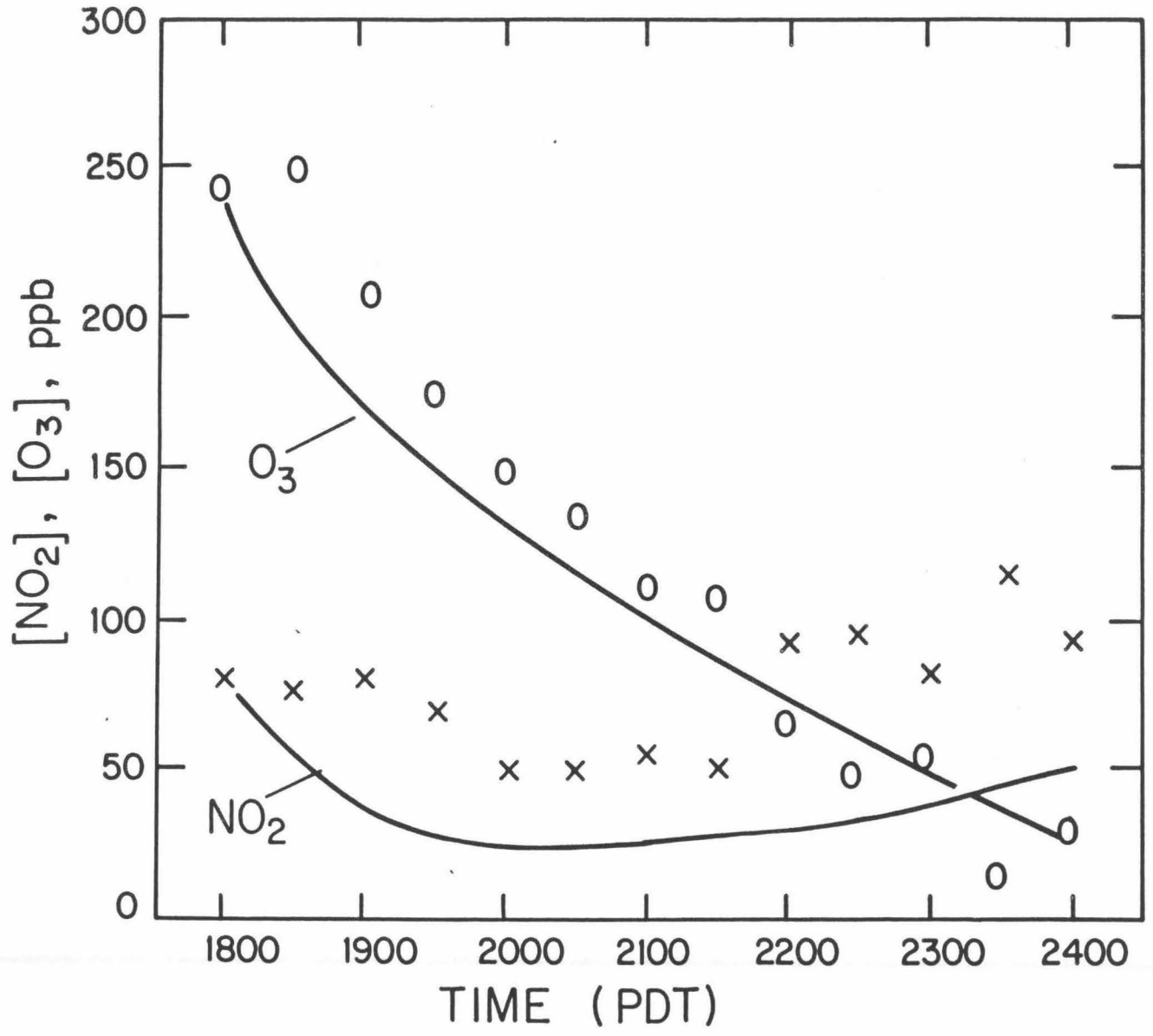
300
250
200
150
100
50
0
[NO2], [O3], ppb
O3
NO2
1800
1900
2000
2100
2200
2300
2400
TIME (PDT)

FIGURE 7

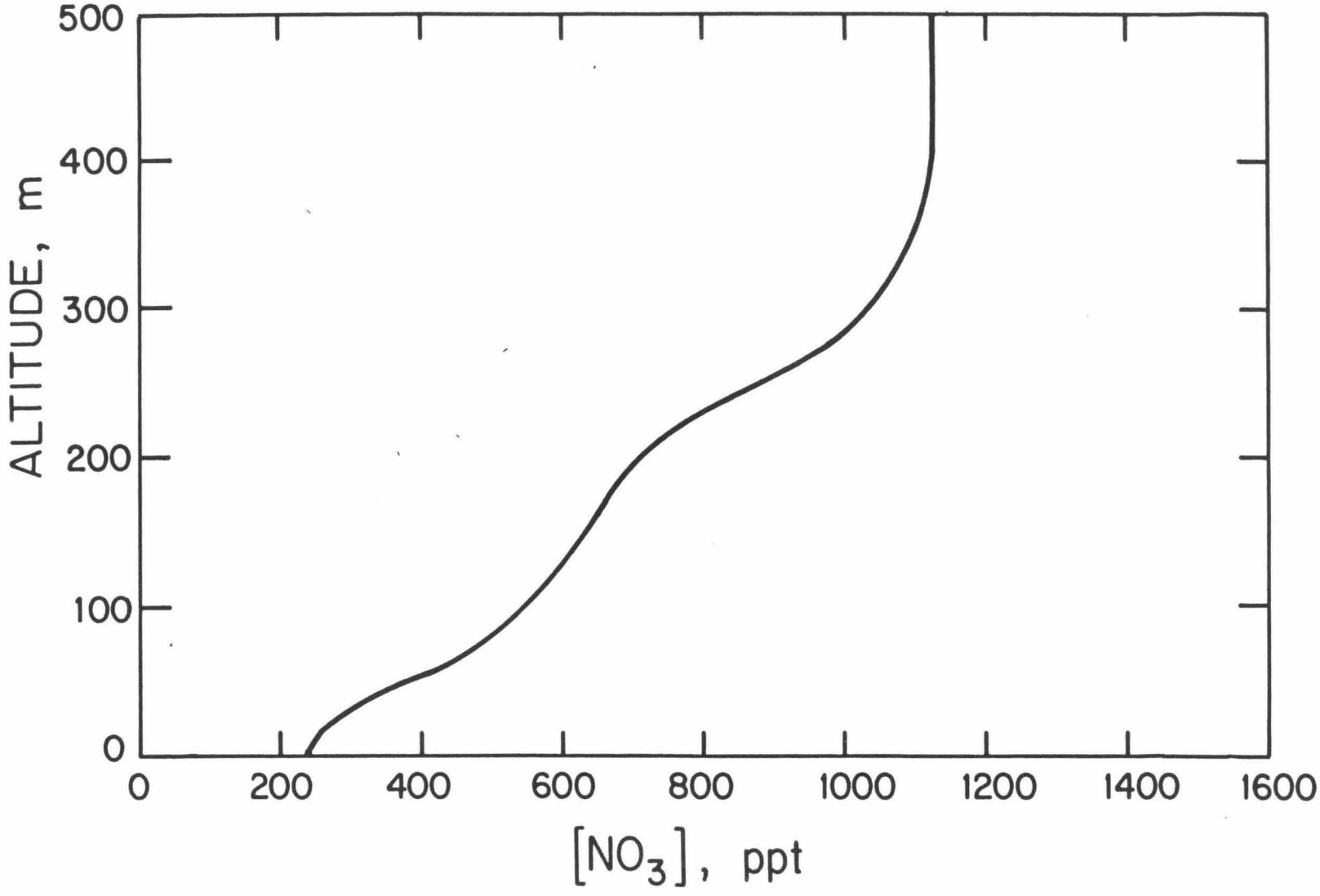
500
400
300
200
100
0
ALTITUDE, m
0
200
400
600
800
1000
1200
1400
1600
[NO3], ppt

FIGURE 8

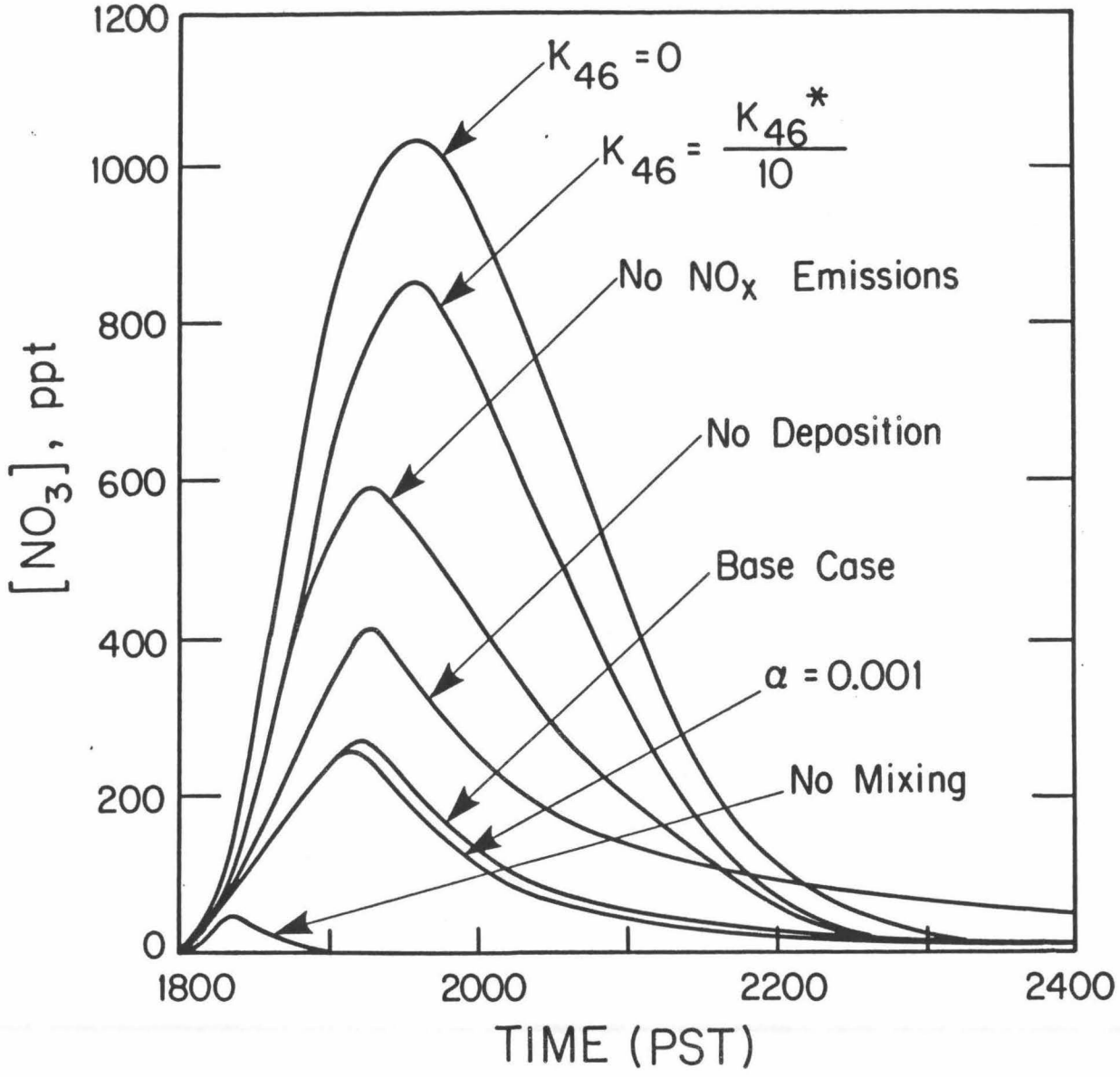
1200
1000
800
600
400
200
0
$[NO_3]$, ppt
$K_{46} = 0$
$K_{46} = \frac{K_{46}^*}{10}$
No NO_x Emissions
No Deposition
Base Case
$\alpha = 0.001$
No Mixing
1800
2000
2200
2400
TIME (PST)

FIGURE 9